Development and Evaluation of Online Estimation Methods for a Feedback-Based Freeway Ramp Metering Strategy

Kaan Ozbay, Ph.D.
Associate Professor
Rutgers University, Civil and Environmental Engineering, 632 Bowser Road, Piscataway, NJ 08854-8014
Tel: 732-445-2792
Fax: 732-445-0577
Email: kaan@rci.rutgers.edu

Ilgin Yasar, M.S.
Ph.D. Candidate
Rutgers University, Civil and Environmental Engineering, 632 Bowser Road, Piscataway, NJ 08854-8014
Tel: 732-445-4012
Fax: 732-445-0577
Email: ilgin@eden.rutgers.edu

Pushkin Kachroo, Ph.D.
Associate Professor
Virginia Tech, Bradley Dept. of Electrical & Computer Engineering, 302 Whittemore Hall, Blacksburg, VA 24061-0111
Tel: 540-231-2976
Fax: 540-380-3383
Email: pushkin@vt.edu

Contact Person
Kaan Ozbay, Ph.D.

Word Count is 5500+5 Figures+3 Tables

ABSTRACT

The critical density of a freeway link is subject to changes over time owing to such circumstances as environmental conditions (snow, rain, etc.) and traffic incidents. Because of the critical density's impacts on the performance of some ramp metering strategies that make use of it as a threshold value for control action, it is necessary to trace the real value of the critical density. Hence, methodologies for the online estimation of critical density using the extended Kalman filter (EKF) and Kalman filter (KF) are proposed in this paper. Basically, critical density is chosen as the state variable to be determined using the system output, namely the measurement of traffic flow on the downstream freeway link. These methods are compared with a similar methodology by Smaragdis et al. (2004) using the same traffic conditions implemented in a macroscopic simulation model based on MATLAB. Then, these proposed methods are evaluated in microscopic simulation environments using PARAMICS. In tracing time-dependent changes of real critical occupancy effectively, the results indicate that both methods (using KF and EKF) provide better performance compared with the case where constant critical occupancy is used for all the scenarios tested. Our paper contributes to state of the art by using a novel on-line parameter estimation techniques combined with two different feedback based ramp metering strategies namely ALINEA and MIXCROS and then by testing this new approach in a highly stochastic microscopic simulation environment that can be considered a close representation of real-world conditions.

1. INTRODUCTION AND MOTIVATION

Ramp metering is one of the most beneficial management strategies in alleviating congestion in freeway networks. Success of the online implementation of feedback-based ramp metering strategies such as "mixed-feedback-based" ramp control strategy, namely MIXCROS (Ozbay et al., 2004), and ALINEA (Papageorgiou et al., 1991) depend on many factors, such as the regulator parameter (K_R) and the appropriate choice of meter locations.

In addition to the need for careful calibration of the control parameters, it is important to improve the performance of the ramp control by introducing adaptive techniques that enable the control strategies to respond in real time to changes in control parameters such as jam density and free flow speed.

The performance standard of the local mixed-feedback-based ramp metering strategy, MIXCROS, for instance, is to maintain the density of the downstream section of the freeway close to the critical density (or the set value chosen to be less than the critical density) while taking the on-ramp queue into consideration with the help of selected weight ratios for the freeway and the on-ramp. In this case, achieving a better performance measure means to maintain downstream freeway density close to a set value of critical density. It also involves keeping the length of the on-ramp queue at reasonable levels close to No Control case so that traffic conditions are improved for the overall ramp system.

One important factor is the use of a set (or critical) occupancy (or density) value. This value is dependent on the capacity of the downstream freeway link, to change the control action. Capacity is the maximum hourly rate at which vehicles reasonably can be expected to traverse a point or a uniform section (*4*). In ramp metering implementations, the capacity of the downstream freeway link has been treated mostly as a constant parameter. It is determined through observation of two of the primary parameters of traffic flow (flow and density). If it is possible to match a best-fit parabolic curve to the entire data set both for stable and unstable flows, the capacity can be estimated as the extreme point of this parabola. Smaragdis et al. (2004) argue that this procedure of critical occupancy determination may not be feasible or fully satisfactory under certain conditions. For instance, the occurrence of congestion on the upstream locations of the network can lead to reduced freeway traffic flow. Therefore, downstream locations of the network may never reach critical occupancy. In such a case, critical occupancy cannot be determined for these locations.

Furthermore, capacity is not a constant value. The stochastic nature of the capacity of a freeway link can be attributed to the variability of traffic characteristics. Changing traffic flow (including traffic conditions and driver behavior), traffic composition, and "external" parameters such as the geometry and environmental conditions of the section all play a role. Adverse weather, for example, clearly affects both the flow-occupancy and speed-flow relationships. Therefore, maximum observed flows (at critical occupancy) usually decrease during adverse weather (*5*). When the critical occupancy is selected to be less than its real value, control laws tend to behave in such a conservative manner that they lead to excessive usage of on-ramp storage. This causes unwanted increases in on-ramp travel time. On the other hand, selecting higher occupancy thresholds results in higher volume and delay on the freeway, causing unwanted mainline delays. Thus, implementing ramp metering strategies using online estimation of critical occupancy ensures better performance.

A strategy that automatically adapts to the real-time change of critical occupancy, based on the freeway traffic conditions at the bottleneck locations, can prove efficient. Similar studies are reported in the literature (e.g., (*6*), (*7*), (*8*), (*9*), (*10*)). In (*7*), a general approach to the real-time estimation of the complete traffic state in freeway stretches is developed based on the extended Kalman Filter (EKF). The EKF has also been applied in the past to obtain improved density estimates ((*8*), (*9*)) by coupling the detector counts with independent density estimates, which are subject to uncorrelated errors. In (*10*), the EKF is employed for estimating vehicle counts for two roadway sections in tandem.

Smaragdis et al. (2004) develops a new strategy. It allows for the automatic tracking of the critical occupancy whenever it cannot be estimated beforehand or whenever it is subject to real-time change as a result of environmental conditions or traffic composition. The aim is mainstream flow maximization.

In this paper, a similar but more efficient method to achieve the same objective is proposed. The effectiveness of method is then evaluated using PARAMICS implementation of ALINEA and MIXCROS.

2. MODEL DETAILS

2.1. The Process Model

The equations in this section are given for the merge segment of Figure 1.

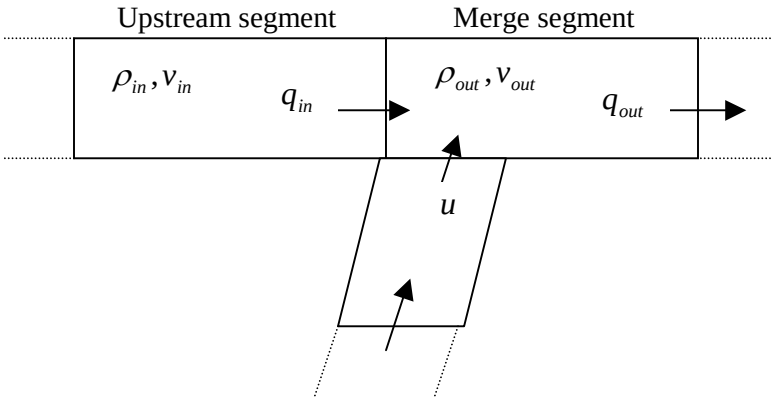

FIGURE 1 Ramp system (upstream segment, merge segment, and ramp link).

Various static and dynamic models have been used to represent the underlying relationship between speed v and density ρ of a freeway section. One of the simplest models is the one proposed by Greenshields (1935) ($v = v_f(1-\rho/\rho_{jam})$), which hypothesizes a linear relationship between the two variables. By combining Greenshields model and the fundamental relationship for traffic flow ($q_{out} = \rho v$), a nonlinear relationship between critical density ($\rho_{cr} = \rho_{jam}/2$) and downstream freeway flow q_{out} is obtained (1):

$$q_{out} = v_f \rho (1 - \frac{\rho}{\rho_{jam}}) \quad (1)$$

where v_f is the free flow speed, and ρ_{jam} is the jam density.

Smaragdis et al. (2004) present an extremum-seeking feedback-control problem, including significant external disturbances and various constraints. The method uses real-time measurements of $q_{out}(k-1), o_{out}(k-1)$ and attempts to produce estimates of prevailing traffic occupancy $\tilde{o}_{cr}(k)$, at which the freeway flow q_{out} is maximized.

Basically, a derivative $D = dq_{out}/do_{out}$ is first calculated at the $(k-1)^{th}$ estimate of $\tilde{o}_{cr}$. If the derivative is sufficiently positive or negative, the new estimate $\tilde{o}_{cr}(k)$ is obtained by adding or subtracting; respectively, an increment Δ to the current estimate $\tilde{o}_{cr}(k-1)$ (Figure 2). However, if the derivative is approximately zero, the new estimate $\tilde{o}_{cr}(k)$ is set equal to $\tilde{o}_{cr}(k-1)$. According to Smaragdis et al. (2004), the algorithm works properly when the time period for calculating the new critical occupancy estimates is a multiple of the time period for updating the metering rate.

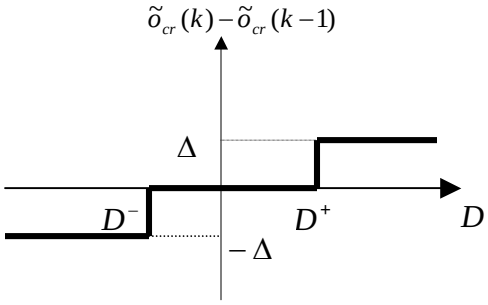

$$\tilde{o}_{cr}(k)=\tilde{o}_{cr}(k-1)+\begin{cases}\Delta & \text{if } D>D^+\\ -\Delta & \text{if } D<D^-\\ 0 & else\end{cases}$$

FIGURE 2 Adaptation function for $\tilde{o}_{cr}$ (Smaragdis et al., 2004).

The estimated derivative can be calculated using two alternative methods. The first method is simple derivative estimation with exponential filter application. The derivative D is estimated at each time step by calculating the following (*1*):

$$\delta(k)=\Delta q_{out}(k-1)/\Delta o_{out}(k-1) \tag{2}$$

where $\Delta.(k-1)=.(k-1)-.(k-2)$ are time differences of the involved measurements. Then, derivative D is estimated by applying an exponential filter

$$D(k)=\alpha\delta(k)+(1-\alpha)D(k-1) \tag{3}$$

where $\alpha\in(0,1)$ is a constant smoothing parameter.

The second method is the derivative estimation based on the Kalman Filter (KF). Real-time measurements of $q_{out}(k-1)$ and $o_{out}(k-1)$ are used to recursively calculate the derivative D around the current estimate $\tilde{o}_{cr}$ by fitting a straight line equation:

$$q_{out}=D(o_{out}-\tilde{o}_{cr})+E \tag{4}$$

The complete algorithm for each approach is given in Smaragdis et al. (2004).

2.2. The Filter Equations and Parameters for the Online Estimation Method Using Extended Kalman Filter

In this section, the use of the EKF is proposed for capturing the time-dependent changes in the value of critical density employed in ramp metering control law equations.

The main idea behind the EKF-based estimation of critical density is to employ critical density directly as the state variable to be filtered using downstream freeway flow measurements.

Let $k=1,2,...$ index time; $k=1$ refers to the initial time. Let us assume that the process has a state parameter ρ_{cr}, which is governed by the stochastic difference equation:

$$\hat{\rho}_{cr}(k)=f(\hat{\rho}_{cr}(k-1),\xi(k-1)) \tag{5}$$

with a measurement q_{out} that is

$$\hat{q}_{out}(k)=f(\hat{\rho}_{cr}(k),\theta(k)). \tag{6}$$

It is assumed that the state changes according to the stochastic difference equation (7):

$$\hat{\rho}_{cr}(k)=A(t)\hat{\rho}_{cr}(k-1)+\xi(k) \tag{7}$$

Here, for simplicity, it is further assumed that $A(t)=1,\ \forall t=1$. The measurement model that describes the relationship between the state and the measurements is presented in the observation equation below:

$$\hat{q}_{out}(k)=v_f\rho(k)\left(1-\frac{\rho(k)}{\hat{\rho}_{jam}}\right)+\theta(k) \tag{8}$$

where from the fundamental relationship $\hat{\rho}_{jam}=2\hat{\rho}_{cr}$, $\xi(k)$ and $\theta(k)$ are the system and output noise, respectively, whose covariance matrices will determine the tracking properties of the resulting EKF (*10*).

It is assumed that ξ and θ have a zero mean and that they are independent of each other, white, and with normal probability distributions:

$$p\{\xi(k)\} \approx N(0, \Xi(k)), \quad (9)$$
$$p\{\theta(k)\} \approx N(0, \Theta(k))$$

where Ξ is the process noise covariance and Θ is the measurement noise covariance.

Here, the a priori estimate at step k is defined as the estimate given knowledge of the process prior to step k and is denoted by a superscript minus sign. In other words, $\rho_{cr}^{-}(k)$ stands for the priori estimate of $\rho_{cr}(k)$. Of course, one does not know the individual values of the noises ξ and θ at each time step. However, one can approximate the state and measurement without ξ and θ, respectively, as

$$\hat{\rho}_{cr}^{-}(k) \cong f(\hat{\rho}_{cr}(k-1), 0) \quad (10)$$
$$\hat{q}_{out}^{-}(k) \cong f(\hat{\rho}_{cr}^{-}(k), 0)$$

Therefore, using (7), (8), and (10), the a priori estimate of state and measurement can be written as:

$$\hat{\rho}_{cr}^{-}(k) \cong \hat{\rho}_{cr}(k-1) \quad (11)$$

$$\hat{q}_{out}^{-}(k) \cong \hat{q}_{out}(\hat{\rho}_{cr}^{-}(k)) \cong v_f \rho(k)(1 - \frac{\rho(k)}{(2 \times \hat{\rho}_{cr}^{-}(k))}) \quad (12)$$

where $\hat{\rho}_{cr}(k)$ and $\hat{\rho}_{cr}^{-}(k)$ are the a posteriori and a priori estimates of state, respectively. $P(k)$ and $P^{-}(k)$ are the a posteriori and a priori state estimation error covariance matrices, respectively, such that

$$P(k) = E\{(\rho_{cr}(k) - \hat{\rho}_{cr}(k))(\rho_{cr}(k) - \hat{\rho}_{cr}k))'\}, \quad (13)$$
$$P^{-}(k) = E\{(\rho_{cr}(k) - \hat{\rho}_{cr}^{-}(k))(\rho_{cr}(k) - \hat{\rho}_{cr}^{-}(k))'\} \quad (14)$$

where $\rho_{cr}(k)$ is the actual state parameter. It is clear from (8) that a nonlinear relationship exists between the state and measurement variable. Therefore, EKF can be used. EKF applies the standard KF to nonlinear systems with additive white noise by continually updating a linearization (a linear Taylor expansion of the system; i.e., the first two terms of the approximation) around the previous state estimate, starting with an initial prediction.

Hence, the new filter equations that linearize an estimate around the previous estimate of the state are the following:

State equation is assumed to be linear:

$$\rho_{cr}(k) \approx \hat{\rho}_{cr}(k) = \hat{\rho}_{cr}(k-1) + \xi(k) \quad (15)$$

Because the measurement equation is nonlinear (8), the new governing equation for the measurement that linearizes an estimate about the a priori estimate of the state (11) is

$$q_{out}(k) \approx \hat{q}_{out}(\hat{\rho}_{cr}^{-}(k)) + H(k)(\hat{\rho}_{cr}(k) - \hat{\rho}_{cr}^{-}(k)) + \Gamma\theta(k) \quad (16)$$

where $H(k)$ is the partial derivative of measurement equation (8) with respect to state variable $\hat{\rho}_{cr}$ at the a priori estimate $\hat{\rho}_{cr}^{-}(k)$.

$$H(k) = \partial\hat{q}_{out}(k)/\partial\hat{\rho}_{cr}(k)\big|_{\hat{\rho}_{cr}(k)=\hat{\rho}_{cr}^{-}(k)} \quad (17)$$

$$H(k) = \frac{V_f \rho^2(k)}{2\hat{\rho}_{cr}{}^2(k)}\bigg|_{\hat{\rho}_{cr}(k)=\hat{\rho}_{cr}^{-}(k)} = \frac{V_f \rho^2(k)}{2\hat{\rho}_{cr}^{-}{}^2(k)} \quad (18)$$

And Γ is the partial derivative of the measurement equation with respect to $\theta(k)$:

$$\Gamma = \partial\hat{q}_{out}(k)/\partial\theta(k)\big|_{\hat{\rho}_{cr}(k)=\hat{\rho}_{cr}^{-}(k)}. \quad (19)$$

It is assumed that the new measurement noise $\Gamma\theta(k)$ has approximately the following distribution

$$p(\Gamma\theta(k)) \approx N(0, \Gamma\Theta(k)\Gamma^T) \quad (20)$$

where Γ^T is the transpose of Γ.

2.2.1 Estimation Algorithm for Critical Density $\hat{\rho}_{cr}$ Using Extended Kalman Filter

EKF methodology for the online estimation of the critical density of a freeway link is given as follows (*10*).

1. Assume that the initial state $\hat{\rho}_{cr(0)}$ is a random variable with known mean and covariance matrix P_0. Initialize the filter by setting the state variable (ρ_{cr}) and the covariance matrix, namely

$$\hat{\rho}_{cr}(0) = x_0, \; P(0) = P_0 \tag{21}$$

2. Predict the state vector and the covariance matrix using the approximate values from (10) and (14), respectively

$$\hat{\rho}_{cr}^{-}(k) \cong f(\hat{\rho}_{cr}(k-1),0) \tag{22}$$
$$P^{-}(k) \cong P(k) + \Xi(k)$$

where $P^{-}(k)$ is the a priori state estimation error covariance.

3. Compute the Kalman gain matrix $K(k)$:

$$K(k) = P^{-}(k)H^{T}(k)(H(k)P^{-}(k)H^{T}(k) + \Theta(k))^{-1}. \tag{23}$$

4. Update the state variable and its covariance matrix

$$\hat{\rho}_{cr}(k) = \hat{\rho}_{cr}^{-}(k) + K(k)(y(k) - \hat{q}_{out}^{-}(k)) \tag{24}$$

where $y(k)$ is the actual measurement of $q_{out}(k)$, and $\hat{q}_{out}^{-}(k)$ is the approximate estimation, which can be determined using (12). Then, update the covariance matrix of the state variable using (25):

$$P(k) = (1 - K(k)H(k))P^{-}(k). \tag{25}$$

5. Go to step 2 and iterate the algorithm when the updated real-time information is available.

2.3. The Filter Equations and Parameters for the Method Using Kalman Filter

As shown in section 2.2.1, there is a nonlinear relationship between the state parameter, namely the critical density $\rho_{cr}(k)$, and the measurement (freeway downstream flow) $q_{out}(k)$. Hence, EKF was used for the online estimation of the state parameter. However, the state parameter can be replaced by a new term to provide a framework for the KF application for the online estimation of critical density, which eliminates the need for linearization of the measurement equation. This new state parameter is defined as

$$inv\_\hat{\rho}_{cr}(k) = 1/\hat{\rho}_{cr}(k). \tag{26}$$

And the new state variable $inv\_\rho_{cr}(k)$ is governed by the following equation:

$$inv\_\hat{\rho}_{cr}(k) = f(inv\_\hat{\rho}_{cr}(k-1), \xi(k-1)) \tag{27}$$

with a measurement q_{out} that is

$$\hat{q}_{out}(k) = f(inv\_\hat{\rho}_{cr}(k), \theta(k)) \tag{28}$$

where $\xi(k)$ and $\theta(k)$ are the system and output noise.

It is assumed that the state changes according to the stochastic difference equation (29):

$$inv\_\hat{\rho}_{cr}(k) = A(t)inv\_\hat{\rho}_{cr}(k-1) + \xi(k) \tag{29}$$

where it is further assumed that $A(t) = 1, \; \forall t = 1$. With the substitution of the new state parameter, the measurement model that describes the relationship between the state and the measurements becomes:

$$\hat{q}_{out}(k) = v_f \rho(k)(1 - \rho(k)inv\_\hat{\rho}_{cr}/2) + \theta(k). \tag{30}$$

The above state (29) and measurement (30) equations have the following linear form:

$$x(k) = x(k-1) + \xi(k) \tag{31}$$
$$y(k) = H(k)x(k) + d(k) + \theta(k) \tag{32}$$

where

$$x(k) = inv\_\rho_{cr}(k),$$
$$y(k) = q_{out}(k),$$
$$H(k) = -v_f \rho^2(k)/2,$$
$$d(k) = v_f \rho(k).$$

It is obvious from (29) and (30) that these new filter equations give linear dynamics and a linear (albeit time varying) measurement equation, which is the framework for standard KF. Therefore, there is no need for an extended version whose results in general are not theoretically as complete as those of the standard ones (*10*).

It is assumed that ξ and θ have a zero mean and they are independent of each other, white, and with normal probability distributions:

$$p\{\xi(k)\} \approx N(0,\Xi(k)), \qquad (33)$$
$$p\{\theta(k)\} \approx N(0,\Theta(k))$$

where Ξ is the process noise covariance and Θ is the measurement noise covariance.

Here, the a priori estimate at step k is defined as the estimate given knowledge of the process prior to step k and is denoted by a superscript minus sign. In other words, $inv\_\rho_{cr}^{-}(k)$ stands for the a priori estimate of $inv\_\rho_{cr}(k)$.

One can approximate the state and measurement without ξ and θ, respectively, because the individual values of the noise ξ and θ at each time step are not readily known. Nevertheless,

$$inv\_\hat{\rho}_{cr}^{-}(k) \cong f(inv\_\hat{\rho}_{cr}(k-1),0), \qquad (34)$$
$$\hat{q}_{out}^{-}(k) \cong f(inv\_\hat{\rho}_{cr}^{-}(k),0).$$

Therefore, using (29), (30), and (34), the a priori estimate of state and measurement can be written as:

$$inv\_\hat{\rho}_{cr}^{\ -}(k) \cong inv\_\hat{\rho}_{cr}(k-1), \qquad (35)$$

$$\hat{q}_{out}^{-}(k) \cong \hat{q}_{out}(inv\_\hat{\rho}_{cr}^{-}(k)) \cong v_f \rho(k)(1-\rho(k) inv\_\hat{\rho}_{cr}^{-}(k)/2) \qquad (36)$$

where $inv\_\hat{\rho}_{cr}(k)$ and $inv\_\hat{\rho}_{cr}^{-}(k)$ are the a posteriori and a priori estimates of state, respectively.

$P(k)$ and $P^{-}(k)$ are a posteriori and a priori state estimation error covariance matrices, respectively, such that

$$P(k) = E\{(inv\_\rho_{cr}(k) - inv\_\hat{\rho}_{cr}(k))(inv\_\rho_{cr}(k) - inv\_\hat{\rho}_{cr}k))'\},. \qquad (37)$$
$$P^{-}(k) = E\{(inv\_\rho_{cr}(k) - inv\_\hat{\rho}_{cr}^{-}(k))(inv\_\rho_{cr}(k) - inv\_\hat{\rho}_{cr}^{-}(k))'\} \qquad (38)$$

where $inv\_\rho_{cr}(k)$ is the actual state parameter.

2.3.1 Linear Estimation Algorithm for Critical $\hat{\rho}_{cr}$ (Method Using Kalman Filter)

KF methodology for the online estimation of the critical density of a freeway link is given as follows (*10*).

6. Assume that the initial state $inv\_\hat{\rho}_{cr(0)}$ is a random variable with known mean and covariance matrix P_0. Initialize the filter by setting the state variable (inv_ρ_{cr}) and the covariance matrix, namely
$$inv\_\hat{\rho}_{cr}(0) = x_0, \ P(0) = P_0 \qquad (39)$$
7. Predict the state vector and the covariance matrix using the approximate values from (34) and (38), respectively
$$inv\_\hat{\rho}_{cr}^{-}(k) \cong f(inv\_\hat{\rho}_{cr}(k-1),0), \qquad (40)$$
$$P^{-}(k) \cong P(k) + \Xi(k)$$
where $P^{-}(k)$ is the a priori state estimation error covariance.
8. Compute the Kalman gain matrix $K(k)$:
$$K(k) = P^{-}(k)H^{T}(k)(H(k)P^{-}(k)H^{T}(k) + \Theta(k))^{-1}. \qquad (41)$$
9. Update the state variable and its covariance matrix
$$\hat{\rho}_{cr}(k) = \hat{\rho}_{cr}^{-}(k) + K(k)(y(k) - \hat{q}_{out}^{-}(k)) \qquad (42)$$
where $y(k)$ is the actual measurement of $q_{out}(k)$, and $\hat{q}_{out}^{-}(k)$ is the approximate estimation, which can be determined using (36). Then, update the covariance matrix of the state variable using (43):
$$P(k) = (1 - K(k)H(k))P^{-}(k). \qquad (43)$$
10. Go to step 2 and iterate the algorithm when the updated real-time information is available.

3. METHODOLOGY

Although the best way to evaluate ramp metering strategies is the use of microscopic simulation models such as PARAMICS, it is important to first test them in the relatively simpler macroscopic simulation environment. Therefore, evaluation of the adaptive critical density determination will be performed in two phases. The first phase includes the macroscopic testing of the proposed methodology using MATLAB to compare it with a similar methodology by Smaragdis et al. (2004). The testing is conducted under the same traffic scenarios of the ALINEA ramp metering strategy implementation with deterministic and stochastic freeway and ramp demands. The second phase involves evaluating the proposed methodology using a microscopic simulation environment (PARAMICS) on two test networks.

3.1. Evaluation Using Macroscopic Simulation Tool

ALINEA does not consider the on-ramp queue directly; it is therefore handled through overriding restrictive metering rates where the metering rate is set to maximum when the queue reaches a predetermined level. As a result, ALINEA would eventually have difficulty balancing freeway congestion and ramp queues if traffic became heavily congested. Thus, to concentrate only on the mainstream impact of the ramp metering strategy, ramp demand was kept at low values and no queue overriding tactics were used in each scenario tested.

In each scenario, the regulator parameter K_R of ALINEA is chosen to be 240 veh/hr. Also, 90% of the critical occupancy is used as the set (desired) occupancy for all the cases.

Simulation is conducted on a ramp system (Figure 1) consisting of a one-lane (1 mile) freeway link and a one-lane (0.5 mile) ramp link. The mainstream capacity is approximately 1,500 veh/hr/lane and is obtained at density values in the range of 35 to 50 veh/mile/lane. The time discretization step for the ramp metering implementation is equal to 1 min. Simulation duration for each case is 5 hr.

The proposed methodology implementation requires the initial critical density estimate, which can be simply determined from (q_{out}, o_{out}) diagrams. This new methodology is compared with the method proposed by Smaragdis et al. (2004) for their response to sudden (Case 1a) and gradual changes (Case 1b) in the capacity of the freeway downstream link (Figure 1). For each scenario, the parameter values used in the simulation are given in Table 1.

TABLE 1 Parameter Values for Each Case in MATLAB Implementation

Case ID	Freeway Demand (veh/min)	Ramp Demand (veh/mi)	Critical Density (Initial=50) (veh/mi)	Initial Critical Density Estimate	Time Step (T*)	Model Parameters
Case 1a	N (24,25)	N (2,16)	N (45,25) N (30,25)			
Proposed Method (KF and EKF)				40	6x	State Noise: N (0,10) Output Noise: N (0,100)
Smaragdis Method (Simple Derivative)				40	6x	$D^+ = 120, D^- = -40$ $P_1 = 0.14$ $\alpha = 0.4, \Delta = 0.009$
Smaragdis Method (Kalman Filter)				40	3x	$D^+ = 0.65, D^- = -0.14$ $P_1 = 16, \Delta = 0.009$ $Z = [10^2\ 0; 0\ 10^4], W = 10^4$ $X(1) = [0 \quad 29]$
Case 1b	N (24,25)	N (2,16)	N (45,25)- N (30,25)			
Proposed Method (KF				40	4x	State Noise: N (0,10) Output Noise: N (0,100)

and EKF)			
Smaragdis Method (Simple Derivative)	40	4x	$D^+ = 100, D^- = -10$ $P_1 = 0.17$ $\alpha = 0.39, \Delta = 0.005$
Smaragdis Method (Kalman Filter)	40	4x	$D^+ = 0.51, D^- = -0.15$ $P_1 = 13, \Delta = 0.005$ $Z = [65\ 0; 0\ 65^2], W = 65^2$ $X(1) = [0 \quad 29]$

*where T is the multiple of the time period to update metering rate.

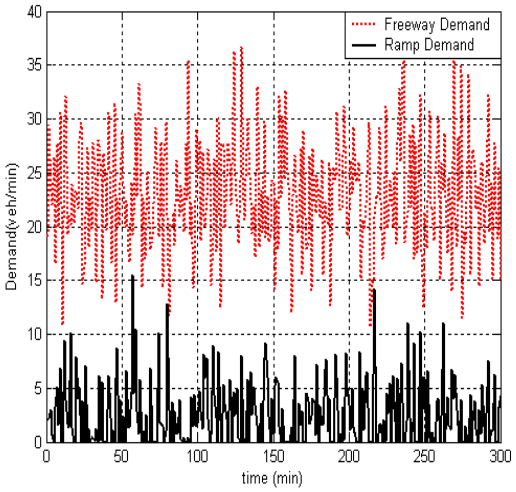

(a)

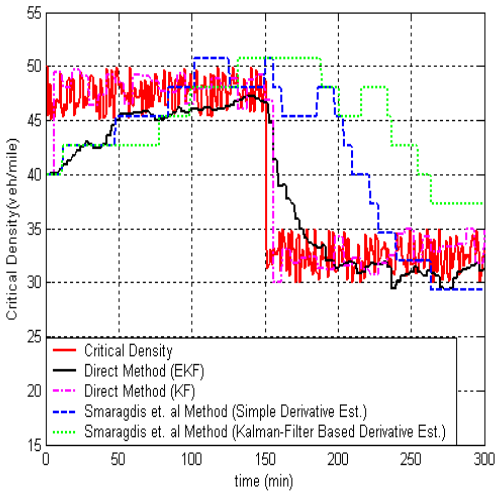

(b)

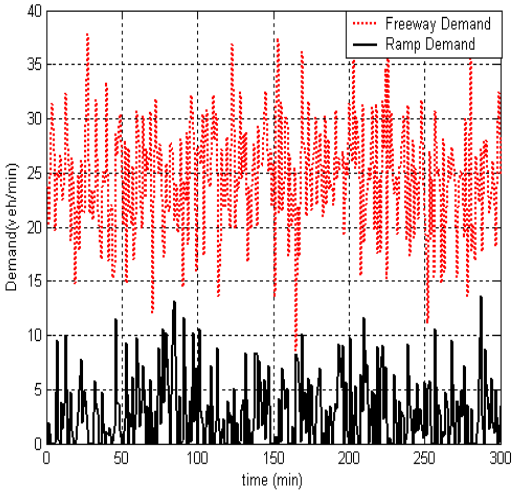

(c)

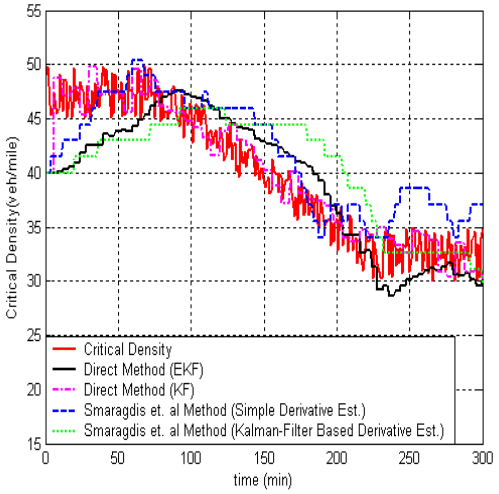

(d)

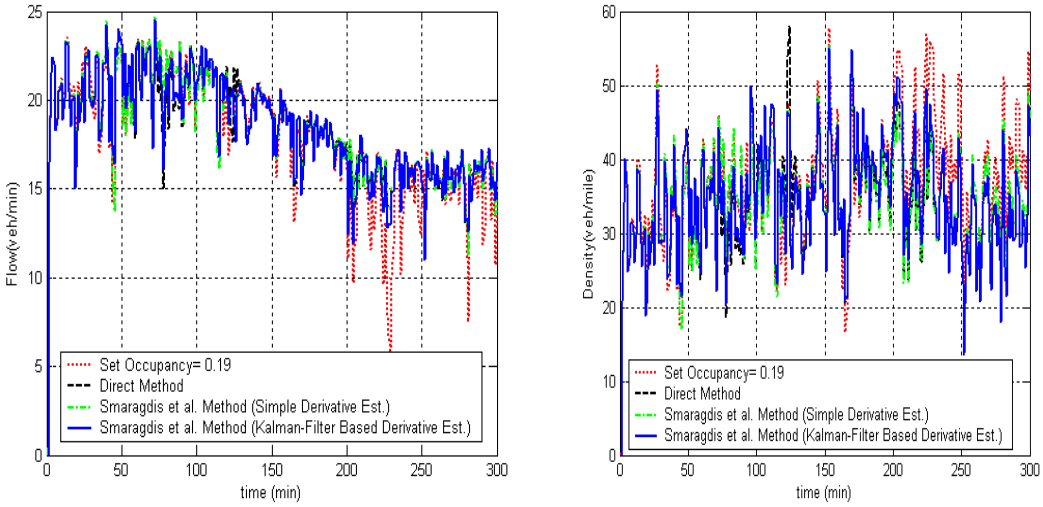

(e) (f)

FIGURE 3 Comparison of the proposed methods with method suggested by Smaragdis et al. (2004) for sudden drop of the critical density (Figures 3a and 3b), gradual drop of the critical density (Figures 3c and 3d), and flow and density vs. time plots for gradual drop of the critical density (Figures 3e and 3f).

In Figure 3, comparison of the proposed methodology with the Smaragdis et al. (2004) method is demonstrated for their ability to successfully trace a gradual and sudden drop of critical density with stochastic demand. To eliminate the positively biased D-estimates, estimation periods are selected to be 3 to 6 times the ramp metering update rate, and asymmetric D^+ and D^- values are used, where $|D^+| > |D^-|$ (Table 1).

The method proposed by Smaragdis et al., both with simple derivative and KF based estimation, is very sensitive to the selection of the parameters. That is, the success of the method largely depends on these values. For instance, testing results in the paper by Smaragdis et al. (2004) show that adaptation works properly for a time step of 1 min (2 times the ramp metering rate update), whereas critical density estimates diverge for a lesser time step. Overall, the method has good adaptive capabilities for tracing gradual change of critical occupancy (Figure 3d). However, it is relatively slow in reacting to sudden changes in the critical density values (Figure 3b). Larger calculation time periods are necessary, and the calibration of the method is quite cumbersome. On the other hand, the proposed methodology (with EKF and KF) performs well in both cases where sudden and gradual changes in critical density at time t = 150 min are observed (Figures 3b and 3d).

In Figures 3e and 3f the downstream flow and density values of each method implementation are compared. Another case where set occupancy is chosen to be constant (19%) is added to the Figure 3e and 3f to observe the impacts of these estimation methods on the ramp system. In these Figures, all the estimation algorithms are shown to maximize the traffic volumes, while reducing the density of the merge section, by tracking real critical density.

3.2. Evaluation Using PARAMICS Microscopic Simulation Tool

Two test networks (Figure 4a and 5) are used for the microsimulation-based evaluation study on the performance of two local traffic-responsive ramp metering strategies, namely, ALINEA and MIXCROS.

Detector data does not include direct section-based density measurements in the real world. Therefore, occupancy readings from the detectors have to be converted to density so as to implement this method.

The first PARAMICS model (Figure 4a) has ten three-lane freeway links (two of which are included in Zones 1 and 2) and four one-lane ramp links (one of which is included in the Zone 3). The speed limit on the freeway is 60 mph. The mean headway and mean reaction time values are 1 sec each, as default. The simulation for each scenario is run for 2 hr. Freeway demand, from Zone 1 to Zone 2 of Figure 3, is 4,320 veh/hr/3 lanes, and ramp

demand is 300 veh/hr. Scatter plots from the PARAMICS model suggest that the downstream freeway link critical occupancy is 21%. There are 4 detectors; two are located on the freeway upstream and downstream, and the rest is located on the ramp upstream and downstream (Figure 4a). Eight scenarios are tested. Four of these use two constant critical occupancy values (the first is an estimate obtained from flow density plots; the second is an arbitrary occupancy value) with ALINEA and MIXCROS, and the last four scenarios use critical density values that are determined using the proposed online estimation methods with ALINEA and MIXCROS. In each ALINEA scenario, the regulator parameter K_R is chosen to be 70 veh/hr. Similarly, in each MIXCROS scenario, the regulator parameter is chosen to be 0.5 (2). The weight ratios for freeway and ramp are selected as 0.5 and 0.5, respectively (2). Of the critical occupancy, 90% is used as the set (desired) occupancy for all the cases. Minimum and maximum green times are chosen as 2 and 15 seconds, respectively. The critical density is determined every minute.

The second test network (Figure 5) is the PARAMICS model of the section of I-295 in South Jersey. The calibrated and validated model of the 3-lane freeway section includes the junctions of I-295 with Route 38, State HWY 73, State HWY 70 and Berlin Rd. In this study, only the southbound traffic is simulated. MIXCROS is implemented on all 4-on-ramps (1-lane each). The length of the corridor from Zone 2 to Zone 1 is 11 mil. The speed limit on the freeway links is 60 mph. Six origin-destination demand zones were created in the network as shown in Figure 5. The proposed methods using KF and EKF are evaluated using three different demand levels in MIXCROS implementation. The congestion levels for each demand level are provided in Table 3a. The congestion level is the percent of the time that the downstream link occupancy is greater than the critical occupancy. Nine scenarios are created, six of which involve the MIXCROS implementation using KF and EKF for three demand levels; the rest involves the MIXCROS implementation using constant critical density, determined through downstream flow density plots. The results are then compared with the No Control case, where no ramp metering control is implemented. All simulations are run for 3 hr with different seed values for the statistical analysis of the results, which ensured a 95% confidence level.

3.2.1. Simulation Results of the First PARAMICS Model

In the No Control scenario, two distinct problem areas, or bottlenecks, are identified from the PARAMICS Modeler simulation viewing of the network and the loop readings obtained from the detectors located on the upstream and downstream of the on-ramp and the freeway. The first area is the freeway downstream link of the ramp system, which is caused not only by the on-ramp traffic but also by a reduction in capacity in the further downstream of the on-ramp (lane drop). This problem area is moving toward the upstream of the ramp system and creating the second problem area, which comprises the on-ramp links. Because there is congestion on the downstream freeway links, the number of vehicles waiting on the ramp is increasing as the number of vehicles released from the ramp into the freeway is decreasing.

Several performance measures are used to evaluate the methodology for the online estimation of critical occupancy (the methods with KF and EKF). The total travel time, ramp system time, and vehicle count values comprise the average of the entire simulation duration. Flow, speed, and density values for the downstream freeway link comprise the average of the loop readings for every 1-min period. Downstream occupancy and on-ramp queues comprise the average of the loop readings for every cycle (17 sec).

Figure 4 shows the comparison of the actual measurement and approximate estimation of downstream flow using KF and EKF. The actual measurement is the flow data obtained from the loop detectors located on the downstream freeway link (Figure 3). The approximate estimation of flow is obtained from the a priori estimate of critical density (Equation (12) in section 2.2 (EKF) and Equation (35) in section 2.3 (KF)).

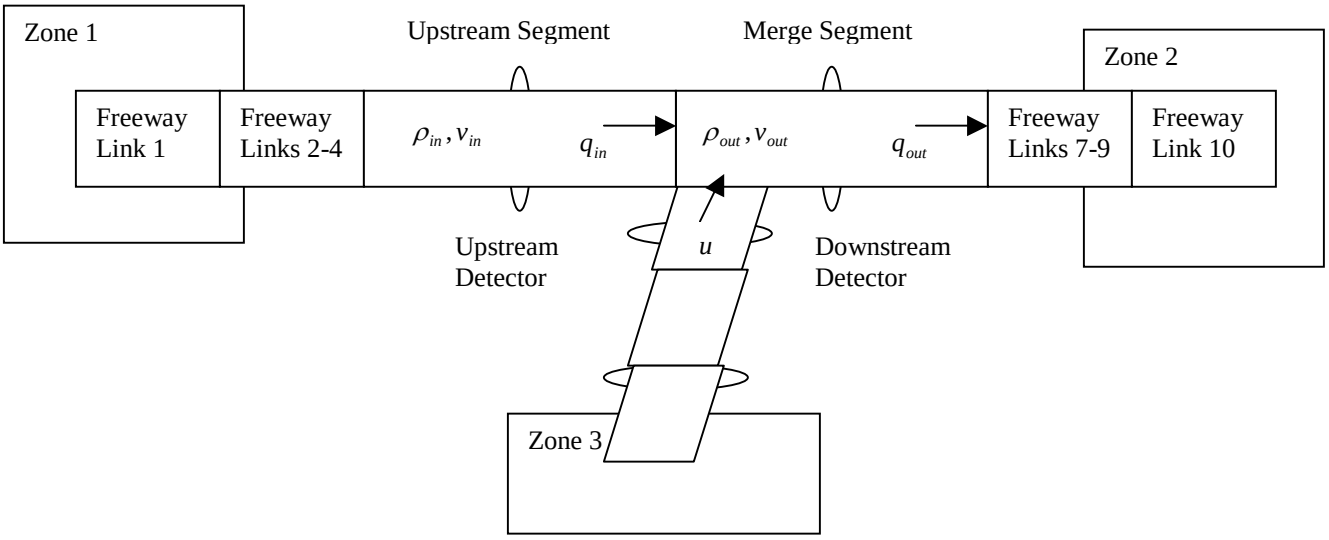
Zone 1
Upstream Segment
Merge Segment
Zone 2
Freeway Link 1
Freeway Links 2-4
ρ_{in}, v_{in}
q_{in}
ρ_{out}, v_{out}
q_{out}
Freeway Links 7-9
Freeway Link 10
Upstream Detector
u
Downstream Detector
Zone 3

(a)

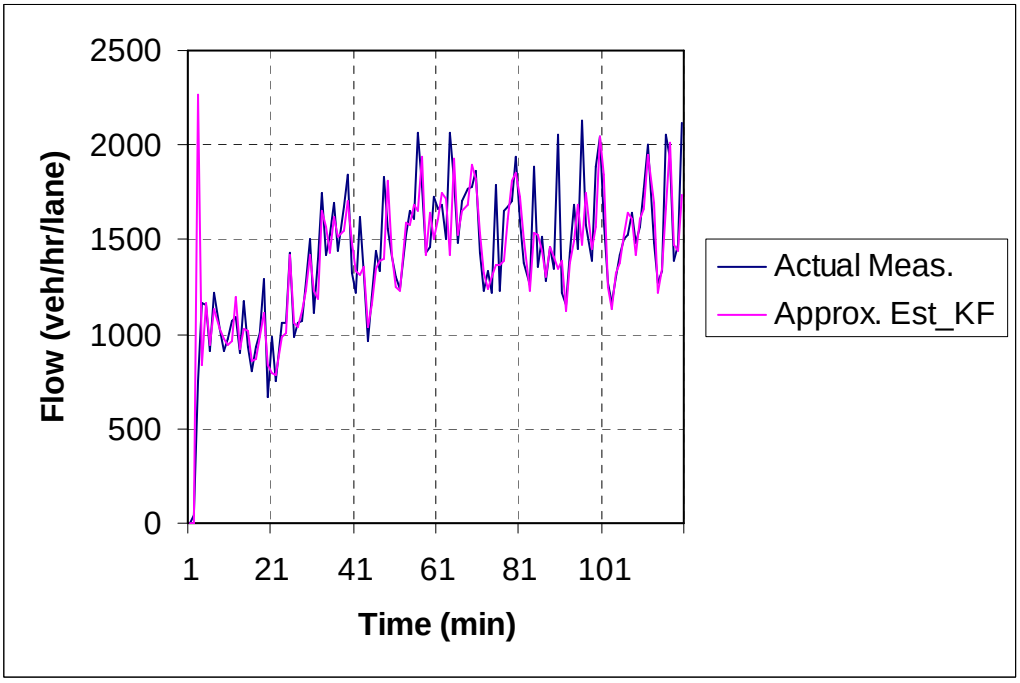
2500
2000
1500
1000
500
0
Flow (veh/hr/lane)
1
21
41
61
81
101
Time (min)
Actual Meas.
Approx. Est_KF

(b)

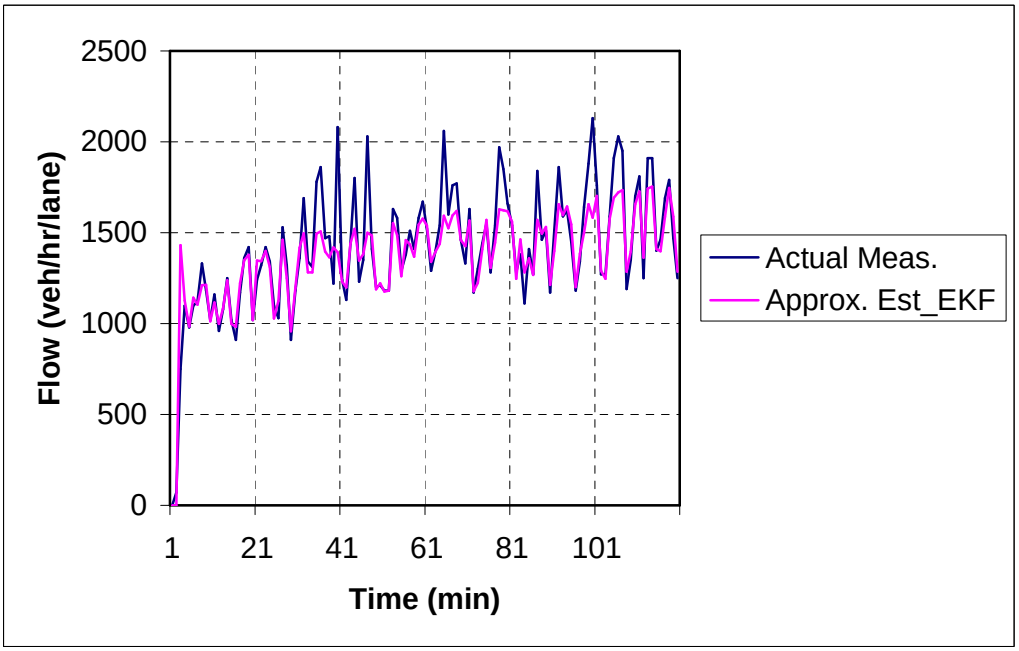
2500
2000
1500
1000
500
0
Flow (veh/hr/lane)
1
21
41
61
81
101
Time (min)
Actual Meas.
Approx. Est_EKF

(c)

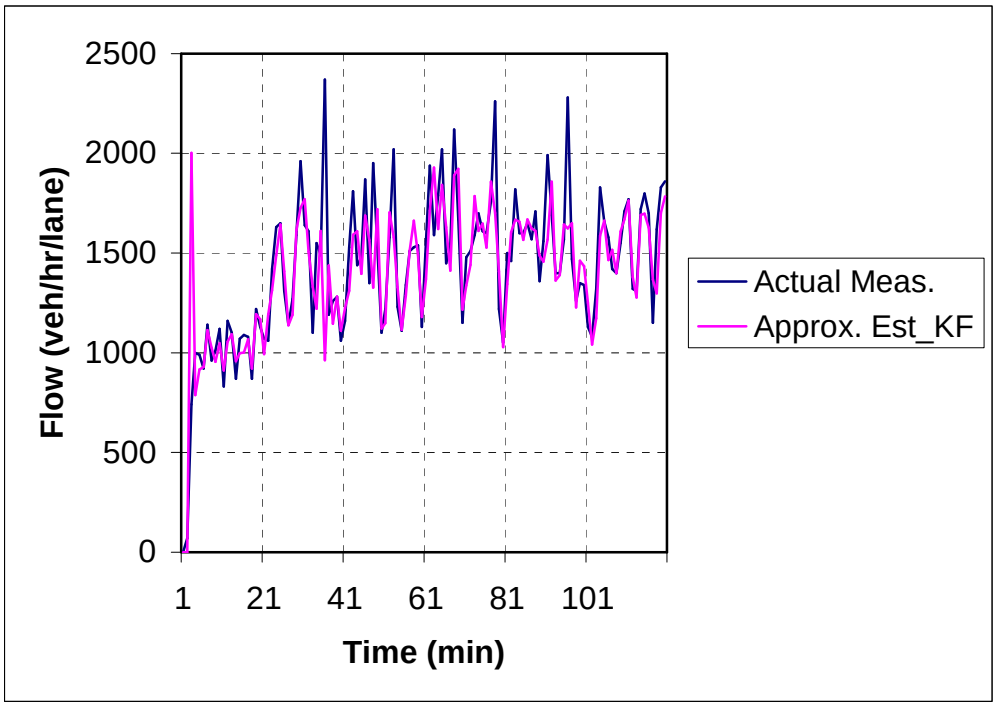
2500
2000
1500
1000
500
0
Flow (veh/hr/lane)
1
21
41
61
81
101
Time (min)
Actual Meas.
Approx. Est_KF

(d)

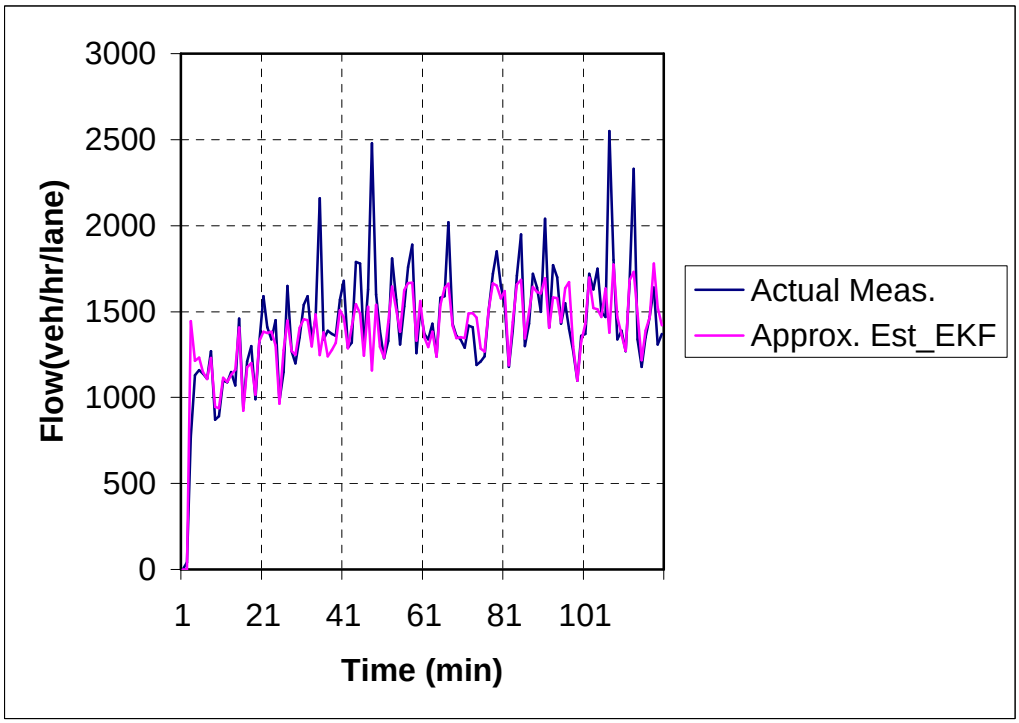

(e)

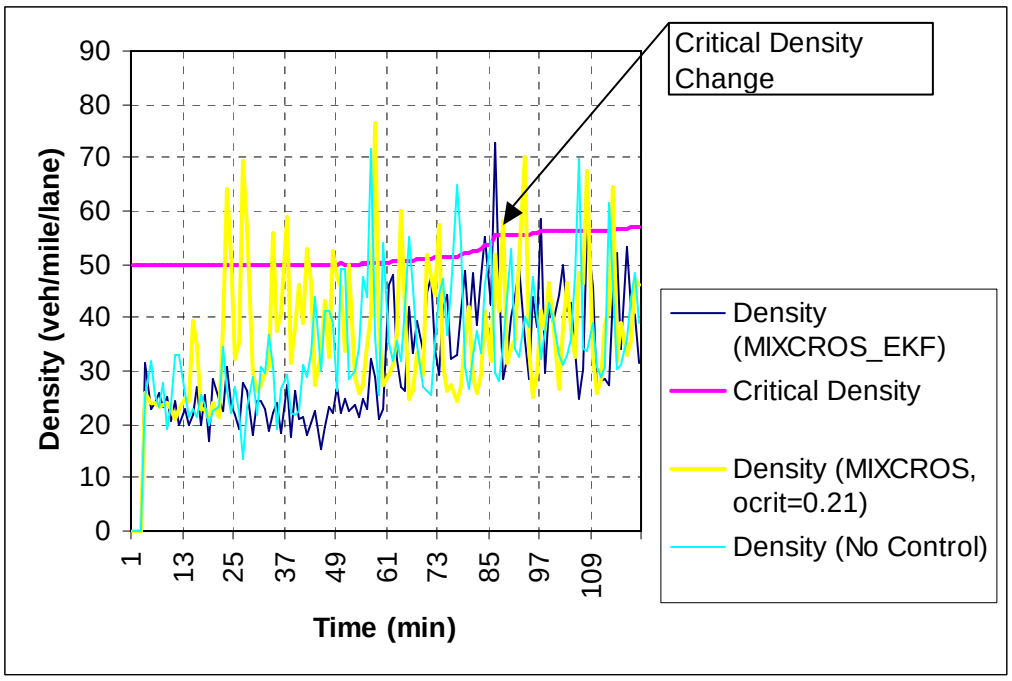

(f)

FIGURE 4 Sketch of PARAMICS model of the system (a); comparison of actual measurement and approximate estimation of downstream flow for MIXCROS (b and c) and ALINEA (d and e) with the proposed method; and comparison of traced critical density and density of the downstream freeway section for the MIXCROS_EKF scenario (f).

Performance measures for all the scenarios are shown in Table 1 (a, b, c, d, e, f). The values in change columns are the percent changes with respect to the No Control scenario. Thus, improvements compared with the No Control are indicated by negative values for the measures of performance (i.e., total travel time, ramp system time, average on ramp queue, average downstream occupancy, and density). On the other hand, positive values are the improvements for average downstream link speed, average downstream freeway link flow, and total vehicle count.

The simulation results show that well-calibrated ramp metering strategies with online estimation of critical occupancy (both methods with KF and EKF) generated up to 36% savings in ramp system travel time (where the ramp system consists of upstream and merge segment, as well as the ramp link between upstream and downstream detectors on the ramp of Figure 3) and up to 24% travel time savings in total network over the 2-hr peak period (Table 1 (a, b)).

TABLE 2a Total Travel Time, Ramp System Time, and Downstream Vehicle Count for ALINEA Scenarios

	Total Travel Time (sec/veh)	Change (%)	Ramp System Time (sec/veh)	Change (%)	Count	Change (%)
No Control	685.65		396.72		7907	
ALINEA_EKF	547.38	-20.17	254.12	-35.94	7910	0.04
ALINEA_KF	589.06	-14.09	281.02	-29.16	7866	-0.52
ALINEA ($\hat{o} = 0.21$)	548.94	-19.94	288.79	-27.21	7893	-0.18
ALINEA ($\hat{o} = 0.25$)	602.39	-12.14	286.16	-27.87	7889	-0.23

TABLE 2b Total Travel Time, Ramp System Time, and Downstream Vehicle Count for MIXCROS Scenarios

	Total Travel Time (sec/veh)	Change (%)	Ramp System Time (sec/veh)	Change (%)	Count	Change (%)
No Control	685.65		396.72		7907	
MIXCROS_EKF	520.94	-24.02	252.22	-36.42	7922	0.19
MIXCROS_KF	572.10	-16.56	273.42	-31.08	7939	0.40
MIXCROS ($\hat{o} = 0.21$)	574.82	-16.16	268.84	-32.23	7887	-0.25
MIXCROS ($\hat{o} = 0.25$)	617.14	-9.99	324.37	-18.24	7932	0.32

TABLE 2c Average On-ramp Queues and Average Downstream Occupancies for ALINEA Scenarios

	Avg. Queue (veh/cycle)	Change (%)	Avg. Down. Occ. (%)	Change (%)
No Control	17		14.38	
ALINEA_EKF	5	-70.59	14.48	0.70
ALINEA_KF	8	-52.94	14.52	0.97
ALINEA ($\hat{o} = 0.21$)	6	-64.71	14.35	-0.21
ALINEA ($\hat{o} = 0.25$)	8	-52.94	14.71	2.29

TABLE 2d Average On-ramp Queues and Average Downstream Occupancies for MIXCROS Scenarios

	Avg. Queue (veh/cycle)	Change (%)	Avg. Down. Occ. (%)	Change (%)
No Control	17		14.38	
MIXCROS_EKF	7	-58.82	13.76	-4.31
MIXCROS_KF	8	-52.94	14.45	0.49
MIXCROS ($\hat{o} = 0.21$)	7	-58.82	14.82	3.06
MIXCROS ($\hat{o} = 0.25$)	12	-29.41	14.04	-2.36

TABLE 2e Average Downstream Flow (3 lanes), Speed, and Density for ALINEA Scenarios

	Avg. Down. Flow (veh/hr/3 lanes)	Change (%)	Avg. Down. Speed (mi/hr)	Change (%)	Avg. Down. Density (veh/mi)	Change (%)

No Control	4261.99		30.85		63.12	
ALINEA_EKF	4323.80	1.45	31.33	1.55	62.66	-0.74
ALINEA_KF	4294.80	0.77	29.98	-2.83	64.29	1.85
ALINEA ($\hat{o} = 0.21$)	4306.09	1.03	29.07	-5.76	65.55	3.84
ALINEA ($\hat{o} = 0.25$)	4277.84	0.37	28.48	-7.69	66.16	4.81

TABLE 2f Average Downstream Flow (3 lanes), Speed, and Density for MIXCROS Scenarios

	Avg. Down. Flow (veh/hr/3 lanes)	Change (%)	Avg. Down. Speed (mi/hr)	Change (%)	Avg. Down. Density (veh/mi)	Change (%)
No Control	4261.99		30.85		63.12	
MIXCROS_EKF	4313.25	1.20	33.91	9.90	58.72	-6.98
MIXCROS_KF	4330.37	1.60	29.97	-2.85	64.35	1.94
MIXCROS ($\hat{o} = 0.21$)	4277.31	0.36	28.62	-7.21	66.94	6.05
MIXCROS ($\hat{o} = 0.25$)	4274.41	0.29	31.56	2.30	62.07	-1.66

Owing to the congestion-relieving affects of the ramp metering strategies on the downstream of the ramp system, the average number of vehicles on the ramp decreased compared with the No Control scenario. With the decrease in downstream congestion, the on-ramp was able to release more vehicles onto the downstream section of the freeway without disrupting downstream traffic.

The average on-ramp queue lengths on the ramp are quite similar for all the scenarios with all tested ramp metering strategies (Tables 1a and 1b). However, MIXCROS was able to improve the entire ramp system without using a queue threshold on the ramp. In ALINEA implementation, a queue constraint of 35 vehicles was used to prevent the occurrence of on-ramp queue spillover into adjacent arterial traffic. The queue override helped avoid large travel time increases (observed in a number of time periods during simulation runs with different seeds). These results were consistent with the results reported in Ozbay et al. (2004).

MIXCROS and ALINEA ramp metering strategies were able to generate some improvements regardless of whether constant or online critical occupancy values were used. However, these improvements were comparatively less for the scenarios with constant critical occupancy. ALINEA performed best with the average critical occupancy (21%) observed from the scattered plots of density. Inaccurate estimation of critical occupancy led to increase in the downstream freeway link occupancy. Average pre-determined critical occupancy implementation of ALINEA was still able to provide improvements in the ramp system and total network time. However, these improvements were less than those obtained from ALINEA with the online critical occupancy strategy. Also, average downstream occupancy was decreased by 4.31% when MIXCROS was implemented using the proposed method with EKF, whereas the same ramp metering strategy was able to decrease the same measure by only 2.36 % with constant critical occupancy (Tables 1c and 1d). It is important to emphasize that for different demand levels, the improvements owing to ramp metering will definitely change. This is a well-reported result by Brilon et al. (2005) (*14*). High levels of improvement in our case can be attributed to the relatively low level of demand given the available capacity. As clearly stated in (*14*), this combination of a relatively low level of demand and a high capacity enhances the performance of ramp metering because of the low percentage of breakdowns observed under heavy traffic conditions.

Mainline volume was increased by 1.6% with MIXCROS using online estimation of critical occupancy (KF) (Tables 1e and 1f). MIXCROS implementation with the proposed method (using EKF) resulted in an approximately 9.9% increase in the average speed in the mainline traffic compared with the No Control scenario; on the other hand, MIXCROS with a constant critical density threshold provided a 2.3% increase in the same performance measure.

In Figure 4 (b, c, d, e) the traced critical density and density of the downstream freeway section are compared for the MIXCROS_EKF scenario. According to this figure, the use of the proposed method led to a decrease in the fluctuations of the density compared with the No Control and constant critical density scenarios. The effects are more visible (Figure 4) when the critical density is subject to change.

The results of microscopic simulation of two distinct ramp metering strategies namely, ALINEA and MIXCROS with the proposed method (KF and EKF) yielded improved traffic conditions not only on the mainline but also on the on-ramp under congested traffic conditions.

3.2.2. Simulation Results of the Second PARAMICS Model

Simulation results of the second PARAMICS model are shown in Table 3 (a through j). The performance measures selected for this section of our study were total travel time (sec/veh) and speed (mi/hr) in the network, average downstream link travel time for each on-ramp (sec/veh), and average queues on each ramp (veh/cycle).

Among the four intersections, MIXCROS is observed to perform better at some intersections, whereas at other intersections, the improvement can be limited. This is because MIXCROS is a local feedback ramp metering strategy. When metering is implemented on one specific ramp using these controls, the traffic conditions on the other ramps are not considered in the metering rates. Therefore, MIXCROS inevitably was not able to provide improvements in all the ramps. On the other hand, implementation of the proposed methods helped MIXCROS provide overall network improvements. For example, at 1st and 2nd demand level, MIXCROS with the proposed method using EKF provided approximately 4% decrease in total travel time, whereas MIXCROS with constant critical density led to almost no improvements. At the same demand levels, MIXCROS with the proposed method with EKF also resulted in an approximately 5% increase in average speed in the network (Tables 3b and 3e).

TABLE 3a Congestion Levels on Each Ramp

	1st Ramp	2nd Ramp	3rd Ramp	4th Ramp
1st Demand Level	27%	60%	68%	20%
2nd Demand Level	53%	39%	58%	9%
3rd Demand Level	0%	17%	35%	24%

TABLE 3b Total Travel Time and Mean Speed (1st Demand Level)

	Tot. Travel Time (sec/veh)	Change (%)	Mean speed (mi/hr)	Change (%)
No Control	646.80		55.00	
MIXED_EKF	620.90	-4.00	57.40	4.36
MIXED_KF	628.55	-2.82	56.68	3.05
MIXED (constant $\hat{o}$)	640.98	-0.90	55.63	1.14

TABLE 3c Average Downstream Link Travel Time for Each On-ramp (1st Demand Level)

	Avg. Downs. Link Travel Time (sec/veh) (1st Ramp)	Change (%)	Avg. Downs. Link Travel Time (sec/veh) (2nd Ramp)	Change (%)	Avg. Downs. Link Travel Time (sec/veh) (3rd Ramp)	Change (%)	Avg. Downs. Link Travel Time (sec/veh) (4th Ramp)	Change (%)
No Control	96.29		32.57		60.59		9.91	
MIXED_EKF	91.72	-4.75	28.60	-12.18	55.20	-8.90	9.98	0.66
MIXED_KF	92.33	-4.12	29.64	-9.00	55.95	-7.65	10.13	2.25
MIXED (constant $\hat{o}$)	93.87	-2.52	30.58	-6.12	58.64	-3.21	9.85	-0.58

TABLE 3d Average Queues for Each On-ramp (1st Demand Level)

	Avg. Queue (veh/cycle) (1st Ramp)	Change (%)	Avg. Queue (veh/cycle) (2nd Ramp)	Change (%)	Avg. Queue (veh/cycle) (3rd Ramp)	Change (%)	Avg. Queue (veh/cycle) (4th Ramp)	Change (%)
No Control	0.9		0.8		2		1.05	
MIXED_EKF	1.4	55.56	0.8	0	2.3	15	1	-4.76
MIXED_KF	1.6	77.78	0.9	12.50	2.5	25	1	-4.76
MIXED (constant $\hat{o}$)	1.6	77.78	0.8	0	2.4	20	1	-4.76

TABLE 3e Total Travel Time and Mean Speed (2nd Demand Level)

Demand 2	Tot. Travel Time (veh/sec)	Change (%)	Mean speed (mi/hr)	Change (%)
No Control	713.30		49.60	
MIXED_EKF	684.48	-4.04	52.18	5.19
MIXED_KF	696.53	-2.35	51.38	3.58
MIXED (constant $\hat{o}$)	690.05	-3.26	51.40	3.63

TABLE 3f Average Downstream Link Travel Time for Each On-ramp (2nd Demand Level)

	Avg. Downs. Link Travel Time (sec/veh) (1st Ramp)	Change (%)	Avg. Downs. Link Travel Time (sec/veh) (2nd Ramp)	Change (%)	Avg. Downs. Link Travel Time (sec/veh) (3rd Ramp)	Change (%)	Avg. Downs. Link Travel Time (sec/veh) (4th Ramp)	Change (%)
No Control	120.11		35.67		62.02		10.09	
MIXED_EKF	108.71	-9.49	34.53	-3.19	61.40	-1.00	9.94	-1.49
MIXED_KF	110.61	-7.91	34.57	-3.10	62.21	0.31	10.12	0.30
MIXED (constant $\hat{o}$)	110.21	-8.24	34.67	-2.80	62.04	0.04	10.23	1.36

TABLE 3g Average Queues for Each On-ramp (2nd Demand Level)

	Avg. Queue (veh/cycle) (1st Ramp)	Change (%)	Avg. Queue (veh/cycle) (2nd Ramp)	Change (%)	Avg. Queue (veh/cycle) (3rd Ramp)	Change (%)	Avg. Queue (veh/cycle) (4th Ramp)	Change (%)
No Control	0.9		0.9		2.0		1.1	
MIXED_EKF	1.2	40.62	0.8	-11.11	2.1	5.00	1.0	-9.09
MIXED_KF	1.6	76.64	0.8	-11.11	2.4	20.00	1.0	-9.09
MIXED (constant $\hat{o}$)	1.4	59.99	0.8	-11.11	2.2	10.00	1.0	-9.09

TABLE 3h Total Travel Time and Mean Speed (3rd Demand Level)

	Tot. Travel Time (sec/veh)	Change (%)	Mean speed (mil/hr)	Change (%)
No Control	616.50		57.80	
MIXED_EKF	610.10	-1.04	58.33	0.91
MIXED_KF	612.85	-0.59	58.08	0.48
MIXED (constant $\hat{o}$)	611.60	-0.79	58.25	0.78

TABLE 3i Average Downstream Link Travel Time for Each On-ramp (3rd Demand Level)

	Avg. Downs. Link Travel Time (sec/veh) (1st Ramp)	Change (%)	Avg. Downs. Link Travel Time (sec/veh) (2nd Ramp)	Change (%)	Avg. Downs. Link Travel Time (sec/veh) (3rd Ramp)	Change (%)	Avg. Downs. Link Travel Time (sec/veh) (4th Ramp)	Change (%)
No Control	91.15		27.84		52.51		10.24	
MIXED_EKF	90.64	-0.56	27.70	-0.52	51.36	-2.19	9.83	-4.03
MIXED_KF	90.84	-0.34	27.81	-0.12	51.29	-2.32	9.79	-4.44
MIXED (constant $\hat{o}$)	90.65	-0.55	27.75	-0.32	51.35	-2.22	9.63	-5.93

TABLE 3j Average Queues for Each On-ramp (3rd Demand Level)

	Avg. Queue (veh/cycle)	Change (%)	Avg. Queue (veh/cycle)		Avg. Queue		Avg. Queue	Change (%)

	(1st Ramp)		(2nd Ramp)	Change (%)	(veh/cycle) (3rd Ramp)	Change (%)	(veh/cycle) (4th Ramp)	
No Control	1.0		0.8		1.9		1.1	
MIXED_EKF	1.2	20	0.8	0	2.3	21.05	1.0	-9.09
MIXED_KF	1.5	50	0.8	0	2.4	26.32	1.0	-9.09
MIXED (constant $\hat{o}$)	1.0	10	0.8	0	2.2	15.79	1.0	-9.09

In Table 3a, the congestion level on each ramp for each demand scenario is shown. In the first demand level, the first three intersections had fairly congested conditions compared with the last intersection, which led to fewer vehicles being released toward the fourth intersection. Therefore, fourth intersection had low upstream and downstream occupancy, speed, density and flow and congestion level. This indicates that the improvements by the controls were insignificant on the third demand scenario for this test network (Tables 3h, 3i, and 3j).

As seen from the Tables 3d, 3g, and 3j, MIXCROS kept the on-ramp queues almost the same size because the No control scenario achieved optimal flow on the ramp and decreased the average downstream link travel time on each ramp system for all demand levels (Tables 3c, 3f, and 3i).

Overall, MIXCROS with the proposed method implementation provided the best improvements both in ramp systems and network-wide among all scenarios tested.

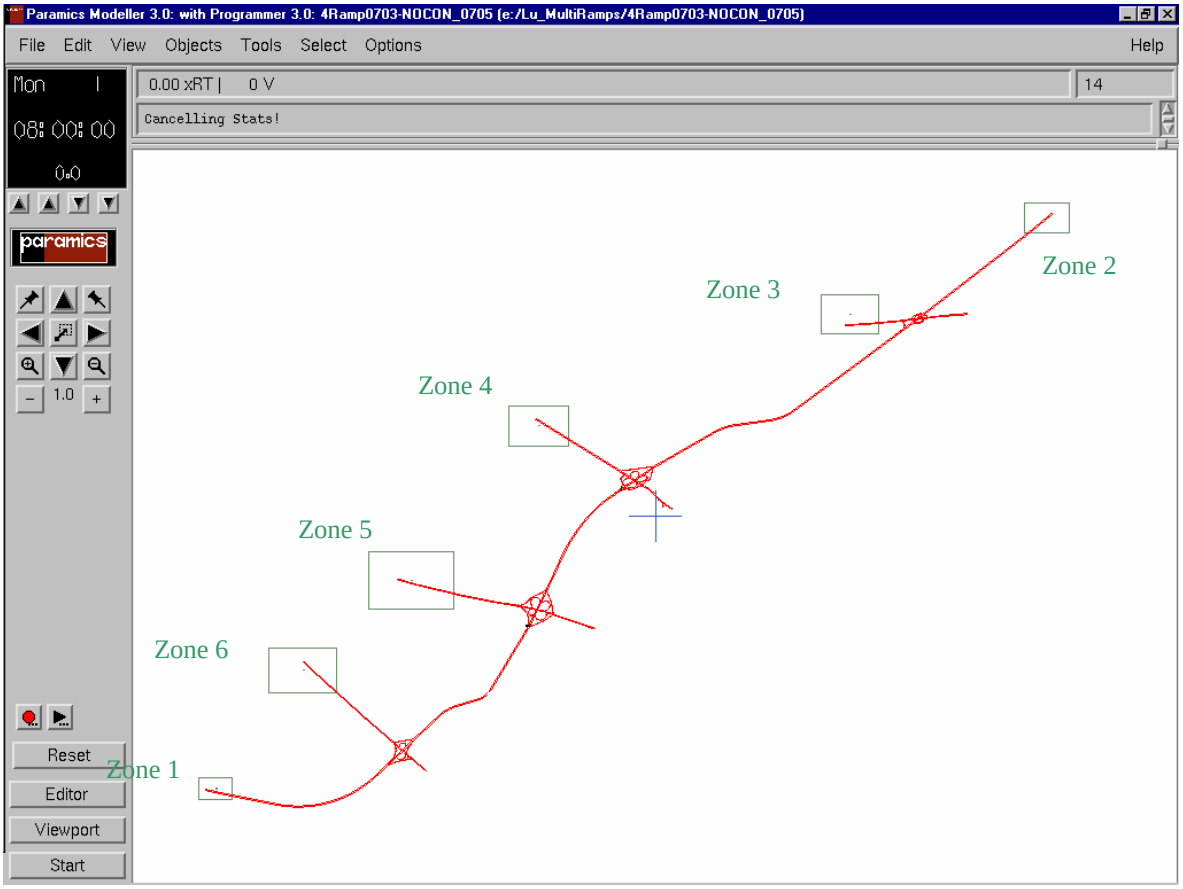

FIGURE 5 Network with 4 on-ramps and 4 off-ramps.

4. CONCLUSIONS

Two new methods are proposed for the online estimation of critical density using EKF and KF; they take the critical density as the state variable to be determined through downstream freeway flow measurements. This new

methodology was tested using both macroscopic (MATLAB) and microscopic (PARAMICS) simulation environments.

Evaluation of the proposed methods show that these methods, unlike the one proposed by Smaragdis et al. (*1*), are not sensitive to the selection of the initial estimate or the time-step size employed to estimate the new critical density. Choice of the initial estimate and time period did not change the adaptive behavior of the methods. Hence, regarding the parameter sensitivity, the proposed methodology is quite robust (*13*). Another strength of the proposed methods is that they respond to sudden capacity changes very well. This can be very valuable during the peak period, when traffic conditions can change unexpectedly ((*13*) and Figure 4).

The proposed online estimation methods using EKF and KF have very simple algorithms. They track very efficiently the change in critical density that can result from environmental conditions, traffic incidents, or simply stochastic fluctuations. The only parameters needed to implement this online estimation methodology are initial estimates of the critical density $\hat{\rho}_{cr(0)}$ and the covariance matrix of the initial state estimate ($\hat{\rho}_{cr(0)}$). The former can be simply determined from the flow density plots. The latter is a random variable with a known mean (Sections 2.2.1 and 2.3.1). The time-step size of the calculations can be assigned any increment of the metering update time, considering that the larger the time-step sizes are, the slower the method converges to the real value of the critical density.

Based on the first microscopic model simulation results obtained from the simple test network shown in Figure 4a, the implementation of ramp metering strategies, namely MIXCROS and ALINEA, on a 4-mile stretch of a 3-lane freeway with one on-ramp significantly decreased the average travel time on the ramp system and the overall network travel times. Improvement in both the ramp system and total network was obtained in the form of reduced average travel time (ramp system and total network), shorter queues on the ramp, and increased throughput on the downstream freeway link. However, these improvements were even greater after the implementation of the proposed online estimation methods.

Microscopic simulation results of both methods using KF and EKF showed approximately the same level of improvement in the ramp system. Both results were superior to the results collected using constant critical density over the course of the simulation. The proposed methods were especially successful at keeping the density at low values, whereas the critical density was subject to changes (Figure 5). They both showed excellent tracking behavior. However, KF is a more desirable approach because it is a linear filter that offers well-known convergence and optimality results. These results can be used to analytically prove the efficiency of ramp metering strategies integrated with it (*11*), a task that will be undertaken in a future paper.

Similarly, based on the second microscopic model simulation results, the proposed methodology showed promise improving the overall system-wide performance of MIXCROS implementation on multiple ramps (e.g., decreasing total travel time and increasing average speed). However, MIXCROS is a local feedback ramp metering control; considering the modifications that allow multi-ramp control, MIXCROS with the proposed on-line parameter estimation methods should perform much better in the networks with such control.

REFERENCES

1. Smaragdis, E., M. Papageorgiou, and E. Kosmatopoulos. A Flow–Maximizing Adaptive Local Ramp Metering Strategy. In *Transportation Research Part B* 38, 2004, pp. 251-270.
2. Ozbay, K., I. Yasar, and P. Kachroo. Comprehensive Evaluation of Feedback Based Freeway Ramp Metering Strategy by Using Microscopic Simulation: Taking Ramp Queues into Account. In *Transportation Research Record*, No. 1867, TRB, National Research Council, Washington, D.C., 2004, pp. 89-96.
3. Papageorgiou, M., H. S. Habib, and J. M. Blosseville. ALINEA: A Local Feedback Control Law for On-ramp Metering. In *Transportation Research Record*, No.1320, TRB, National Research Council, Washington, D.C., 1991, pp. 58-64.
4. Highway Capacity Manual (2000).
5. Ibrahim, A. T., and F. L. Hall. Effect of Adverse Weather Conditions on Speed-Flow-Occupancy Relationships. In *Transportation Research Record*, No.1457, TRB, National Research Council, Washington, D.C., 1994.
6. Yibing, W. and M. Papageorgiou. Real-time Freeway Traffic State Estimation Based on Extended Kalman Filter: A General Approach. In *Transportation Research Part B* 39, 2005, pp. 141-167.
7. Sun, X., L. Munoz, and R. Horowitz. Highway Traffic State Estimation Using Improved Mixture Kalman Filters for Effective Ramp Metering Control. In *Proceedings of the 42nd IEEE Conference on Decision and Control*. Maui, Hawaii, USA, Dec. 9-12, 2003, pp. 6333-6338.

8. Sun, X., L. Munoz, and R. Horowitz. Mixture Kalman Filter Based Highway Congestion Mode and Vehicle Density Estimator and its Application. In *Proceeding of the 2004 American Control Conference*, Boston, Massachusetts, June 30-July 2, 2004, pp. 2098-2103.
9. Szeto, M. W., and D. C. Gazis. Application of Kalman Filtering to the Surveillance and Control of Traffic Systems. In *Transportation Science* Vol. 6(4), 1972, pp. 419-439.
10. Gazis, D., and C. Liu. Kalman Filtering Estimation of Traffic Counts for Two Network Links in Tandem. In *Transportation Research Part B* 37, 2003, pp. 737-745.
11. D. C. Welch, G., and G. Bishop, An Introduction to Kalman Filter, SIGGRAPH 2001-Course 8.
12. Gelb, A. et al. Applied Optimal Estimation, The Analytic Sciences Corporation, 1974, pp.188.
13. Ozbay, K., I. Yasar, and P. Kachroo. Evaluation of Application of Extended Kalman Filtering to Online Estimation of Critical Density, Working Paper, Rutgers Intelligent Transportation systems (RITS) Laboratory, 2005.
14. Brilon, W., J. Geistefeldt, and M. Regler. Reliability of Freeway Traffic Flow: A Stochastic Concept of Capacity. Transportation and Traffic Theory Flow, Dynamics and Human Interaction. In *Proceedings of the 16th International Symposium on Transportation and Traffic Theory*, University of Maryland, College Park, Maryland, 19-21, 2005, July.

LIST OF TABLES

LIST OF FIGURES